Supporting Information

Effects of Nitrate on the Stability of Uranium in a Bioreduced Region of the Subsurface

WEI-MIN WU,[†] JACK CARLEY,[‡] STEFAN J. GREEN,[§] JIAN LUO,[||] SHELLY D. KELLY,[%] JOY VAN NOSTRAND,[#] KENNETH LOWE,[‡] TONIA MEHLHORN, [‡] SUE CARROLL, [‡] BENJAPORN BOONCHAYANANT,[†] FRANK E. LÖFLLER,[||,⊥] DAVID WATSON,[‡] KENNETH M. KEMNER,[%] JIZHONG ZHOU,[#] PETER K. KITANIDIS,[†] JOEL E. KOSTKA,[§] PHILIP M. JARDINE,[‡] AND CRAIG S. CRIDDLE[*,†]

Department of Civil and Environmental Engineering, Stanford University, Stanford, CA 94305; Environmental Sciences Division, Oak Ridge National Laboratory, P.O. Box 2008, Oak Ridge, TN 37831; Department of Oceanography, Florida State University, Tallahassee, FL 32306; [l]School of Civil and Environmental Engineering, Georgia Institute of Technology, Atlanta, GA 30332; Biosciences Division, Argonne National Laboratory, Argonne, IL, 60439; Department of Botany and Microbiology, University of Oklahoma, Norman, OK 73019; School of Biology, Georgia Institute of Technology, Atlanta, GA 30332.

Number of pages = 17, number of Figures = 5; number of Tables = 4.

* Corresponding author phone: (650)723-9032; fax: (650)725-3164; email: ccriddle@stanford.edu
[†]Stanford University, Oak Ridge National Laboratory, [§]Florida State University, [||]School of Civil and Environmental Engineering, Georgia Institute of Technology, [%]Argonne National Laboratory, [#]University of Oklahoma, [⊥]School of Biology, Georgia Institute of Technology

1. Field Test System

The field test system was similar to that described previously (Wu et al., 2006, 2007) with minor modifications. In normal operation, an outer recirculation loop (from FW024 to FW103) is used to protect a nested inner recirculation loop (from FW026 to FW104) from penetration by highly contaminated source zone groundwater. Ethanol additions stimulated reduction of U(VI) to U(IV) in the inner loop. Multilevel sampling (MLS) wells FW100, FW101, FW102, FW107, FW108 and FW109, and monitoring well FW105 and FW110 were used to monitor the geochemistry and microbial community, as shown in FIGURE S1. All recirculation wells and FW105 were of diameter 10.16 cm and a depth of 13.8 m. FW110 was of diameter 1.9 cm and a depth of 10.9 m. MLS FW100, FW101 and FW102 contained seven separate sampling tubes (diameter =1.9 cm; depths =6.10, 7.62, 9.14, 10.67, 12.19, 13.7, and 15.2 m) while two separate sampling tubes were installed in FW107 (13.3 and 14.8 m bgs), FW108 (10.7 and 12.2 bgs) and FW109 (10.6 and 12.2 bgs) with a diameter of 1.9 cm. Wells FW101-2 (sampling at 13.7 m bgs), FW101-3 (12.2 m bgs), FW102-2 (13.7 m bgs) and FW102-3 (12.2 m bgs) were used for routine monitoring because these depth levels had the highest groundwater flow rates, and highest U in the water and on the solid phase during previous tests (Wu et al., 2007).

The recirculation flow rate in both the inner and outer loops was 0.45 L min^{-1}. To minimize entry of ambient groundwater, additional clean water (0.9 L min^{-1}) was injected into FW024 The clean water was Y-12 Plant tap water (pH 8.0 with 2.82 to 3.38 mM chloride; 0.04 to 0.048 mM nitrate; 0.24 to 0.26 mM sulfate; 0.68 to 0.75 mM Ca, < 0.007 mM Al) adjusted pH to 5.5 with HCl. Beginning on day 638, Na_2SO_3 (approximately 0.9 mM) was added to the storage tank. The sulfite removed oxygen by the reaction $2SO_3^{2-} + O_2 \rightarrow 2\ SO_4^{2-}$ and decreased DO to near zero, but did not reduce U(VI). This water was injected into the outer loop injection well FW024. Pulse pumps (QED Environmental Systems, Inc., Ann Arbor, MI) extracted water from wells FW026 and FW103. Metering pumps (Series MP, Pulsafeeder Inc., Punta Gorda, FL) were used to intermittently deliver ethanol and other solutions into the inner or outer loop recirculation line during tests.

Ethanol and its metabolites were monitored as Chemical Oxygen Demand (COD), where 8 g of oxygen demand contains one mole of available electrons. Ethanol, prepared as a 9.8 g COD L^{-1} stock solution, was normally injected at FW104 over a 48-hour period each week, resulting in a COD of 120-150 mg L^{-1} at FW104. A solution of K_2CO_3 (375 mM) was also injected to manipulate pH and carbonate concentrations when needed. Alkalinity at the MLS wells ranged from 0.8 to 4 mM as HCO_3^-, depending on K_2CO_3 additions.

2. Tracer tests

Bromide tracer studies were conducted on Days 1166, 1398 and 1559. A bromide solution was injected into the inner loop injection well FW104. Samples were taken periodically from monitoring wells to determine bromide concentrations. Breakthrough patterns are shown in FIGURE S2. The results indicated that the FW100 well was poorly connected to the inner loop injection well FW104 throughout the test period. Low recovery of Br^- was also observed in FW107, FW109 and FW110 (data not shown). No bromide was observed in FW108. High bromide recovery was observed in FW101-2 (13.7 bgs) and FW102-3 (12.2 m bgs). FW102-2 (13.7 m bgs) received about 50% of water from FW104. High bromide recovery was obtained in FW101-3 but the recovery decreased to a low level on day 1559. The MLS wells at 15.2 m bgs (FW101-1 and FW102-1) and 10.7 m bgs (FW101-4 and FW102-4) were also less connected to FW104, and received low amounts of bromide. The tracer results also indicated that the outer loop was connected to the inner loop. About 10-20% of bromide injected to FW104 was recovered in the outerloop extraction well FW103, depending upon the test period. Using the model developed by Luo et al. (2007), the bromide recovery and mean travel time were estimated for each monitoring well. These data are summarized in TABLE S1.

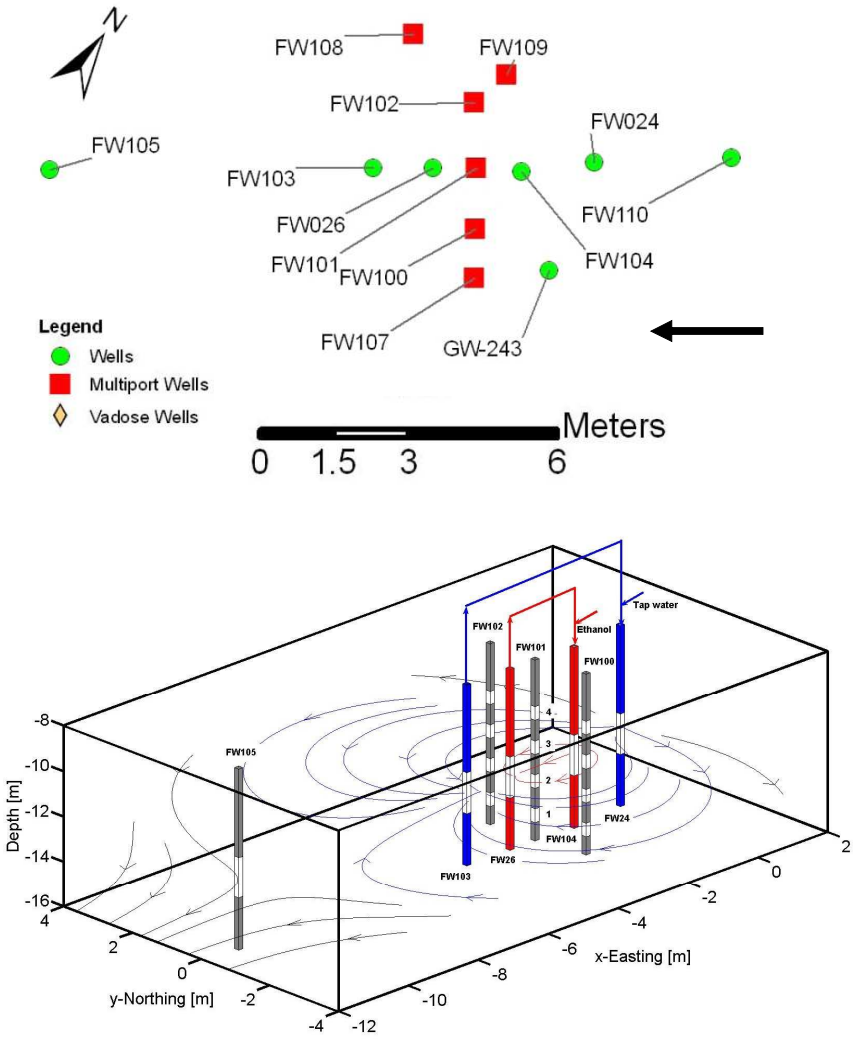

FIGURE S1. Pilot-scale bioremediation well system (above) with expected recirculation patterns (below). Ethanol was injected into the inner loop (red color). Clean water was added to flow entering the outer loop injection well to protect the inner loop from invasion of outside groundwater.

3. Reactions related to this study

The biogeochemical reactions involved in this study are summarized in Table S1.

TABLE S1. Biogeochemical reactions during subsurface reduction & reoxidation and Gibbs free energy changes (at 25°C, pH=7) (data source: Thauer et al., 1977, Lide, 1991)

Reaction Equation	
Coupled U(IV) oxidation reactions	ΔG°', kJ/mol
(1) $UO_{2(s)} + 2/5\ NO_3^- + 12/5\ H^+ \rightarrow UO_2^{2+} + 1/5\ N_2 + 6/5\ H_2O$	-66.2
(2) $UO_{2(s)} + 2/3\ NO_2^- + 8/3\ H^+ \rightarrow UO_2^{2+} + 1/3\ N_2 + 4/3\ H_2O$	-106.9
(3) $UO_{2(s)} + 2Fe^{3+} \rightarrow 2Fe^{2+} + UO_2^{2+}$	-70.32
(4) $UO_{2(s)} + 2Fe(OH)_3 + 6H^+ \rightarrow 2Fe^{2+} + UO_2^{2+} + 6H_2O$	-129.56
Coupled Fe(II) oxidation reactions	
(5) $FeS + 9/5\ NO_3^- + 8/5\ H_2O \rightarrow Fe(OH)_3 + SO_4^{2-} + 9/10\ N_2 + 1/5H^+$	-768.79
(6) $Fe^{2+} + 1/5\ NO_3 + 12/5\ H_2O \rightarrow Fe(OH)_3 + 1/10\ N_2 + 9/5H^+$	-97.87
(7) $Fe^{2+} + 1/3\ NO_2^- + 7/3\ H_2O \rightarrow Fe(OH)_3 + 1/6\ N_2 + 5/3H^+$	-118.32
Nitrate reduction half reactions	ΔG°', kJ/eq
(8) $1/5\ NO_3^- + 6/5\ H^+ + e^- \rightarrow 1/10\ N_2 + 3/5\ H_2O$	-56.18
(9) $½\ NO_3^- + H^+ + e^- \rightarrow ½\ NO_2^- + ½\ H_2O$	-41.65
(10) $1/8\ NO_3^- + 5/4H^+ + e^- \rightarrow 1/8\ NH_4^+ + 3/8\ H_2O$	-45.10
Fe(III), sulfate, and U(VI) reduction half reactions	
(11) $Fe(OH)_3 + 3\ H^+ + e^- \rightarrow Fe^{2+} + 3\ H_2O$	25.17
(12) $1/8\ SO_4^{2-} + 19/16\ H^+ + e^- \rightarrow 1/16\ HS^- + 1/16\ H_2S + ½\ H_2O$	20.85
(13) $½\ UO_2^{2+} + e^- \rightarrow ½\ UO_2(s)$	-39.11
Electron donor oxidation half reactions	
(14) $1/12\ CH_3CH_2OH + 1/4\ H_2O \rightarrow 1/6\ CO_2 + H^+ + e^-$	-31.18
(15) $¼\ CH_3CH_2OH + ¼\ H_2O \rightarrow ¼\ CH_3COO^- + 5/4\ H^+ + e^-$	-37.46
(16) $1/8\ CH_3COO^- + 3/8\ H_2O \rightarrow 1/8\ CO_2 + 1/8\ HCO_3^- + H^+ + e^-$	-26.36
(17) $½HS^- + ½H_2S \rightarrow S + 3/2\ H^+ + e^-$	-51.95
(18) $1/6\ S + 2/3\ H_2O \rightarrow 1/6\ SO_4^{2-} + 4/3\ H^+ + e^-$	-19.19
Precipitation and dissolution of ferrous sulfide	K_{sp}
(19) $FeS_{(s)} \leftrightarrow Fe^{2+} + S^{2-}$	8×10^{-19}
(20) $Fe(OH)_{2(s)} \leftrightarrow Fe^{2+} + 2\ OH^-$	4.87×10^{-17}
(21) $Fe(OH)_{3(s)} \leftrightarrow Fe^{3+} + 3\ OH^-$	2.79×10^{-39}

4. **Results of tracer tests.**

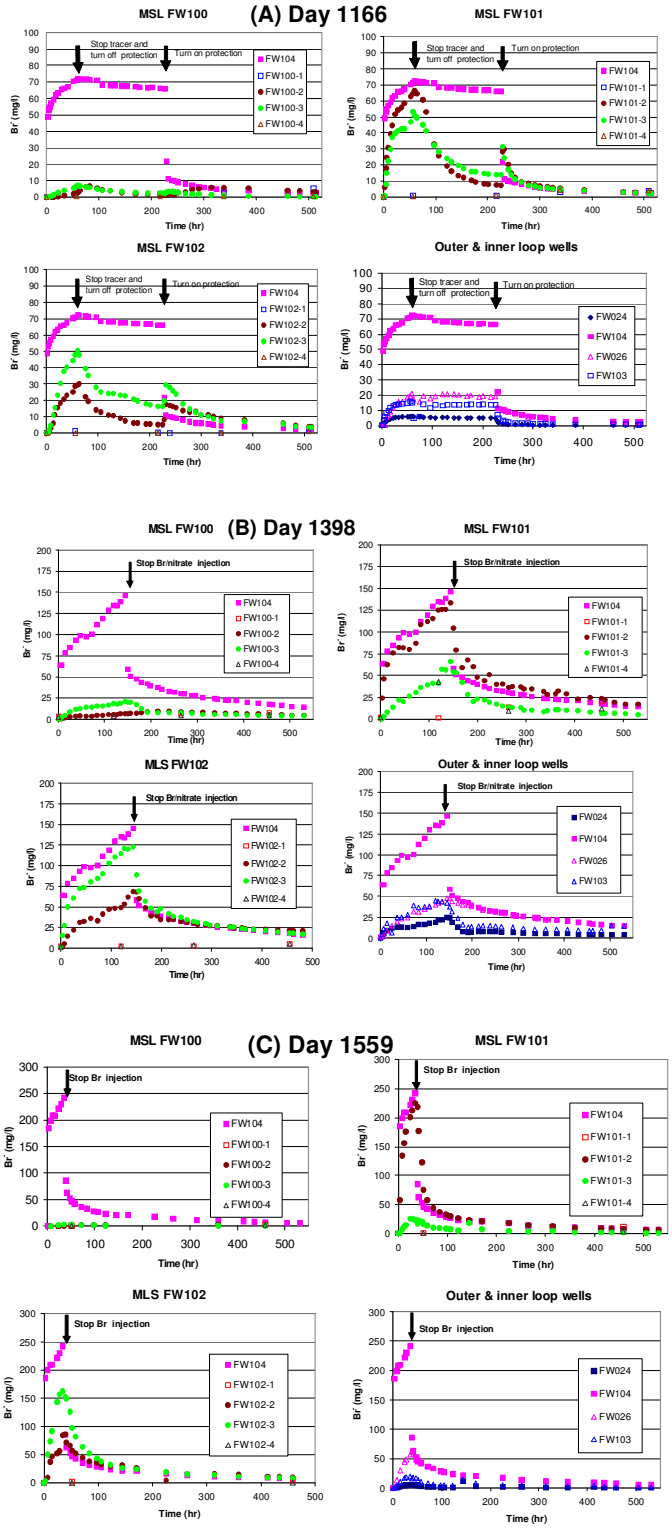

FIGURE S2. Tracer test results on Day 1166 (A), 1398 (B) and 1559 (C).

TABLE S2. Hydraulic connectivity of the inner loop injection well FW104 to the monitoring wells.

		Connectivity of Injection Well to Monitoring Wells Bromide Recovery (%) / Mean Travel Time (h)			
Day	Redox Status	FW101-2	FW101-3	FW102-2	FW102-3
1166	Reduced	92%/7.3 h	70%/7.7 h	41%/106 h	70%/38 h
1398	Oxidized	92%/8.8 h	45%/30 h	47%/79 h	84%/9.6 h
1559	Reduced	93%/6.9 h	9.5%/52 h	36%/74 h	63%/20 h

Bromide tracer tests were conducted on days 1166, 1398 and 1559. FIGURE S2 illustrates changes in bromide concentrations at the injection, extraction, and monitoring wells. The recovery of bromide (%) and mean travel time were calculated using models described elsewhere (Luo et al., 2007), and the results are summarized in TABLE S2.

5. Controlled Nitrate Addition (Days 1398-1419)

An experiment with controlled nitrate addition was performed at FW 104. The flow rates of both the inner and outer loop extraction wells were set to 0.45 L min^{-1}. Water injected at the outer loop injection well FW024 was augmented with 0.9 L min^{-1} of clean water (deoxygenated). The study was executed in four phases:

Phase 1 (Days 1398-1403): Bromide and nitrate were added to the inner loop injection well FW104. On Day 1402, changes in groundwater flowpaths led to an abrupt increase in nitrate concentrations at FW103 with extraction of nitrate-rich source zone groundwater. By Day 1403, nitrate/bromide ratios at FW103 were >18 times those of inner loop extraction well FW026, but this water did not enter the inner loop.

Phase 2 (Days 1403-1404): Nitrate, bromide, and ethanol were added to the inner loop injection well FW104. By the end of Day 1404, nitrate/bromide ratios at FW103 were 142 times those of FW026, indicating continued extraction of nitrate-rich groundwater from the source zone.

Phase 3 (Days 1405-1408): Ethanol alone (no nitrate or bromide) was added to the inner loop injection well FW104. Nitrate concentrations at this well FW104 became very low (0.1 to 0.01 mM). Nitrate levels

at the inner loop extraction well FW026 also decreased to low levels (0.1-0.2 mM), but nitrate concentrations at the outer loop extraction well FW103 remained elevated at 3-7 mM (FIGURE S3B).

Phase 4 (Days 1408-1419): ethanol, nitrate, and bromide additions to the inner loop stopped, but the inner loop extraction well continued to extract and recirculate groundwater. Nitrate concentrations within the inner loop increased slightly, with concentrations at inner loop injection well FW 104 increasing to 0.4 mM by Day 1419.

6. Invasion of nitrate-containing groundwater from the source zone (Days 1420-1496)

From Day 1420 to Day 1434, ethanol was also injected intermittently at the inner loop injection well FW104. Despite the added ethanol, nitrate concentrations increased in the outer loop extraction well FW103, reaching ~20 mM by Day 1428 and in the inner loop injection well FW104 reaching 4 mM by Day 1438 before slowly decreasing (FIGURE S3A). On Day 1451, the groundwater extraction pump in well FW103 was turned off, enabling penetration of source zone groundwater to the inner loop extraction well FW026. Water was extracted at FW026 at a flow rate of 0.45 L min^{-1} augmented with 0.9 L min^{-1} of clean, deoxygenated water then injected into injection well FW104 (29, 30).

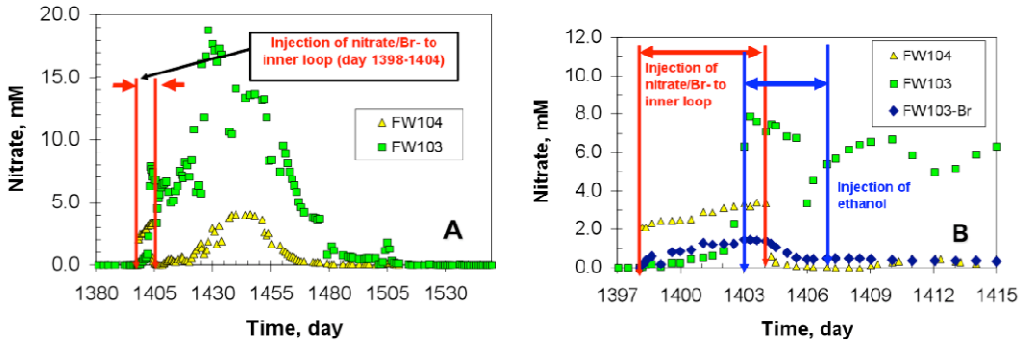

FIGURE S3. (A) Nitrate concentrations at outer loop extraction wells FW103 and inner loop extraction well FW104 throughout the study period (Days 1398-1570) (B) Nitrate and bromide concentrations at the inner loop injection well FW104, FW103 (outer loop) and at the outer loop injection well FW103 during the test of controlled nitrate addition.

7. Bacterial Community Analysis

Genomic DNA was extracted from replicate sediment and surge samples (250 mg) using the Mo Bio PowerSoil™ DNA Isolation Kit (Mo Bio Laboratories, Carlsbad, CA, USA) per the manufacturer's instructions. Surge samples were thawed and centrifuged (20,000g) prior to decanting of the supernatant, and extraction from the sediment phase. For 16S rRNA gene amplification, the 27F and 1492R general bacterial primers (Lane, 1991) were used. PCR reactions were conducted using DreamTaq polymerase and buffer (Lucigen Corporation, Middleton, WI), using 30 reaction cycles at an annealing temperature of 55ºC. Primers were present at a working concentration of 0.5 μM, and the reaction magnesium concentration was 2.0 mM. The PCR yield was column purified using the GenCatch (TM) PCR Cleanup Kit (Epoch Biolabs, Sugar Land, TX, USA). The cleaned PCR yield was ligated into the pSMART® GC HK vector (Lucigen Corporation, Middleton, WI, USA) and *E. coli* were transformed and grown per the manufacturer's instructions. Picked clones were suspended in sterile 0.85% NaCl, and shipped to Sequetech Corporation (Mountain View, CA, USA) for sequencing using the bacterial 16S rRNA gene primer 907R (5'-CCG TCA ATT CMT TTG AGT TT-3'; e.g. Muyzer et al. 1998). Some ligation products were shipped directly to the Washington University - Genome Sequencing Center (St. Louis, MO, USA) for transformation, colony picking and sequencing reactions with plasmid-bound primers. The returned sequences were filtered to remove poor quality data and to remove vector sequence data using the software package Sequencher (Version 4.6, Gene Codes Corporation, Ann Arbor, MI, USA). The sequence data were aligned using the online software package Greengenes (DeSantis et al. 2006) and with the Ribosomal Database Project (RDP) pyrosequence pipeline (Cole et al. 2009). Estimation of diversity indices and classification of sequences were performed using tools at the RDP site (Wang et al. 2007; Cole et al. 2008). Results are summarized in TABLE S3. A threshold of 97% sequence similarity was used for the determination of operational taxonomic units (OTU). A total of 351 clones were analyzed from 4 samples, with 44 to 114 clones per sample. These sequences were submitted to GenBank (National Center for Biotechnology Information; http://www.ncbi.nlm.nih.gov/), under the accession numbers HM146429-HM146779 .

TABLE S3. Bacterial 16S rRNA gene clone library analyses[a].

		FW101-2		FW102-3	
	Total Library	**Day 1202**	**Day 1490**	**Day 1202**	**Day 1490**
Number of Sequences	251	77	44	64	66
Number of OTU[a]	69	23	21	35	23
Shannon Index[b]	3.72 (0.13)	2.67 (0.24)	2.77 (0.27)	3.34 (0.21)	2.81 (0.22)
Taxonomic Classification[c]					
Number of Sequences[d]	351	114	44	105	88
Betaproteobacteria	148 (42%)	55 (48%)	23 (52%)	33 (31%)	37 (42%)
Rhodocyclaceae	68 (19%)	34 (30%)	7 (16%)	17 (16%)	10 (11%)
Hydrogenophilaceae	31 (9%)	9 (8%)	8 (18%)	1 (1%)	13 (15%)
Comamonadaceae	16 (5%)	4 (4%)	2 (5%)	9 (9%)	1 (1%)
Oxalobacteraceae	15 (4%)	2 (2%)	3 (7%)	3 (3%)	7 (8%)
Nitrosomonadaceae	13 (4%)	5 (4%)	2 (5%)	2 (2%)	4 (5%)
Deltaproteobacteria	68 (19%)	30 (26%)	2 (5%)	30 (29%)	6 (7%)
Desulfobacteraceae	25 (7%)	7 (6%)	1 (2%)	14 (13%)	3 (3%)
Geobacteraceae	20 (6%)	14 (12%)	1 (2%)	5 (5%)	0 (0%)
Desulfovibrionaceae	11 (3%)	5 (4%)	0 (0%)	4 (4%)	2 (2%)
Desulfobulbaceae	10 (3%)	4 (4%)	0 (0%)	6 (6%)	0 (0%)
Acidobacteria	36 (10%)	12 (11%)	2 (5%)	6 (6%)	16 (18%)
Bacteroidetes	31 (9%)	3 (3%)	1 (2%)	18 (17%)	9 (10%)
Firmicutes	15 (4%)	1 (1%)	1 (2%)	6 (6%)	7 (8%)
Peptococcaceae	7 (2%)	1 (1%)	1 (2%)	4 (4%)	1 (1%)
Chlorobia	8 (2%)	1 (1%)	7 (16%)	0 (0%)	0 (0%)
Epsilonproteobacteria	7 (2%)	5 (4%)	1 (2%)	1 (1%)	0 (0%)
Other	38 (11%)	7 (6%)	7 (16%)	11 (10%)	13 (15%)

[a] All statistical analyses were conducted using 97% identity as a threshold for OTU determination.

[b] Values in parentheses represent 95% confidence intervals.

[c] Classification was performed using the Ribosomal Database Project (RDP) Classifier

[d] Not all sequences were used for statistical analyses above; therefore sequence numbers are not identical between diversity estimates and classification.

8. **XANES Measurements at MR-CAT**

The XANES analyses were carried out at Argonne National Laboratory (ANL). Samples measured at ANL are shown in Supplemental FIGURE S4. Sediment samples from the wells were collected in anaerobic serum bottles with He or Ar headspace and stored at 4 ^{o}C in a refrigerator. They were centrifuged to separate the sediments from the supernatant within a Coy(R) Anoxic Chamber filled with N_2 and H_2 mixture, mounted under anoxic conditions into plexiglass sample holders with x-ray transparent windows of Kapton film covered with Kapton tape, and stored at 4° C in canning jars filled with anoxic atmosphere for at most 3 days until measurements were made at the MR-CAT (Segre et al., 2000) beamline at the Advance Photon Source, Argonne National Laboratory, USA. The sealed samples were exposed to oxygen only briefly to place them in the sample chamber at the beamline which was purged with N_2 gas. When exposed to atmospheric conditions, sealed samples have been shown to preserve the anoxic integrity of the samples for more than 24 hours (O'Loughlin et al., 2003). The average valence states of U within the moist sediments were measured under anoxic conditions with no pretreatment of the sediments.

The MR-CAT insertion device beamline parameters were as follows. The insertion device was operated on the third harmonic with a taper of approximately 2 keV to produce an incident x-ray intensity as uniform as possible over the scanned x-ray region from 17,000 eV to 18,000 eV. A double crystal Si(111) monochromator was used to select the x-ray energy. A Rh harmonic x-ray rejection mirror was used to eliminate x-rays with higher harmonic energies. The x-ray profile at the sample was approximately 0.7 mm square. The incident, transmitted, and fluorescence x-ray intensities were measured with pure N_2, mixture of 90% N_2 and 10% Ar, and pure Ar filled ionization chambers, respectively. The fluorescence ionization chamber was used with solar slits and an Al filter in the Stern-Heald geometry (Stern et al, 1979). Linearity tests of the experimental setup performed with 50% attenuation in x-ray intensity on reference samples indicated that the nonlinearity in the detectors was less than 0.5% (Kemmer et al., 1994). A energy reference spectrum from a hydrogen uranyl phosphate

standard was measured with each energy scan. This reference was measured after the sample using a reference ionization chamber filled with a mixture of 90% Ar and 10% N_2.

The monochromator was scanned continuously to collect quick spectra within ~ 2 minutes. Long x-ray exposure times to the moist samples showed some changes in the XANES spectra. Therefore two scans, resulting in less than 5% change in the spectra were collected from many different regions of the uniform sample consisting of fine particulates surged from the wells. The spectra from each sample were averaged to increase the signal to noise ratio within the final spectra. The averaged spectra are shown in FIGURE S4.

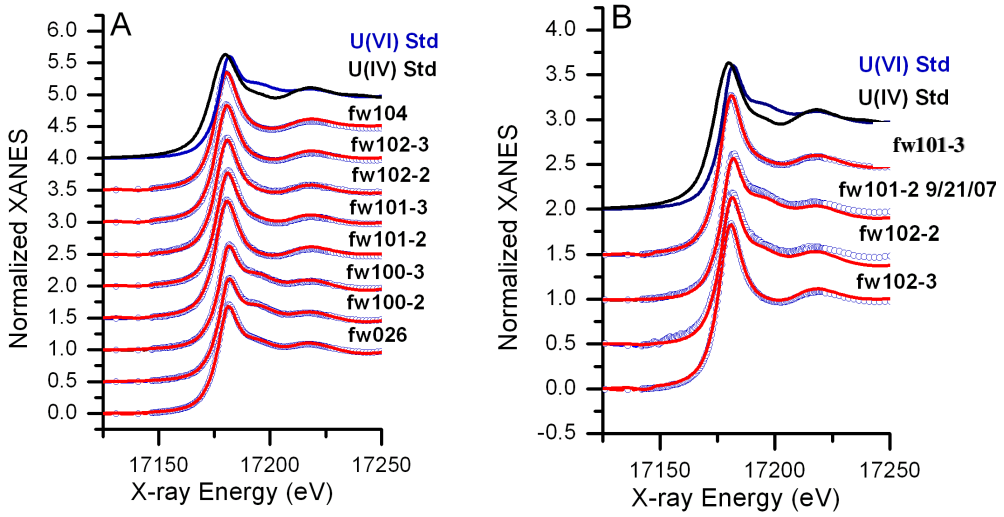

FIGURE S4. XANES analysis of selected samples (blue circle) and linear combination fitting (red line) with one example of U(IV) (black line) and U(VI) standards (blue line). A. Sediment samples on day1202. B. Sediment samples on day 1490. Data of day 1578 are not shown.

The XANES spectra were modeled with a linear combination of standard spectra with the software Athena (Ravel et al., 2005) which uses IFEFFIT methods (Newville, et al., 2001). Two different

U(VI) and U(IV) spectra were used as possible standards as needed to reproduce the measured spectra. The U(VI) standards are aqueous uranyl nitrate at low pH (denoted U(VI) Std-1) and a hydrogen uranyl phosphate mineral (denoted U(VI) Std-2). The U(IV) standards are a natural uraninite mineral (denoted U(IV) Std-1) and abiotically produced uraninite particles (denoted U(IV) Std-2) (O'Loughlin, et al., 2000). These standards are shown in FIGURE S4.

The linear combinations are shown with the measured spectra in FIGURE S4. The average U(IV) percentage is listed in TABLE 1 in the paper with the remaining percentage as U(VI). As shown in FIGURE S4, the XANES spectra depend largely on the U valence state but also to a lesser extent on U speciation. The reference spectra used in the linear combination fitting are from species that may be different from the actual species within the sediment samples, causing some systematic error in the percentage of U(IV) to U(VI) within the sediment sample. Based on the differences of the XANES spectra for different U(VI) and U(IV) species, we generously estimate the accuracy of this method to be 10%.

9. Sampling methods for groundwater and sediments

Groundwater was pumped directly from wells to 45-ml glass bottles, allowing overflow of at least 3-4 exchanges of the bottle volume. The bottles were crimp-sealed with Teflon-coated rubber septum then transferred to a onsite trailer laboratory for analysis of pH, COD, Fe(II), nitrite, ammonium, alkalinity (as HCO_3^-) and sulfide. The samples for metal and KPA analysis were transferred to a 2-mL plastic centrifuge tube, acidified with 0.03 mL 12N nitric acid and sealed for metal and KPA analysis. One milliliter samples for gas chromatography (GC) analyses were acidified with 0.3 M oxalic acid and sealed in 1.5-mL GC vial. Samples for IC analyses (nitrate, sulfate and chloride) were supplemented with K_2CO_3 solution (0.2 ml, 2.0 M) in a 20-mL sanitation tube to remove Al, Fe and Ca from the aqueous phase prior to IC analyses. DO and temperature were measured directly using a HACH D10 DO meter in wells.

To collect sediment samples from injection, extraction and monitoring wells, a PVC surge block (10 x 15 cm for 10.16 cm ID wells and 1.8x 5 cm for 1.9 cm ID wells) was attached to a threaded rod and

inserted into the well to the depth of a targeted 1.0-m well screen. The block was lifted up and down 4 to 5 times in a rapid plunging motion, with a 2 m stroke. The plunging motion detached sediment from the soil matrix surrounding the screen and sucked it through the screen into the well. The sediment settled to the bottom of the well. The loose sedient was then pumped to the surface, collected in 2-liter glass bottles under Ar or He gas phase, and sealed with butyl rubber stoppers. For XANES analyses, a sediment sample was then extracted from the settled slurry layer using a 25-mL glass pipette, transferred to a 27-mL anaerobic pressure tube or a 135-mL serum bottle capped with a butyl rubber stopper, then crimp-sealed with a aluminum cap within an anaerobic glove bag. Additional supernatant was removed by syringe, leaving a volume of supernatant that was generally less than one third the total volume. The headspace of the pressure tube or serum bottle was flushed with He or Ar. For microbial analysis, the slurry was transferred to the laboratory and centrifuged at 3,000 rpm to separate sediment from water. The pellets were frozen in a 60 mL plastic tube at -80 ^{o}C prior to shipping on dry ice to Florida State University and University of Oklahoma.

10. Temperature change during the test period

FIGURE S5 shows changes in groundwater temperature in wells FW103 and FW026 during the test period. The temperatures in these extraction wells varied from 13 to 21 ^{o}C over 580 days. Re-oxidation experiments with nitrate were conducted in the summer of 2007 (2, 3 and 4 in FIGURE S5) while temperatures ranged from 18 to 21 ^{o}C; re-reduction experiments were performed in the autumn and winter when groundwater temperatures were lower.

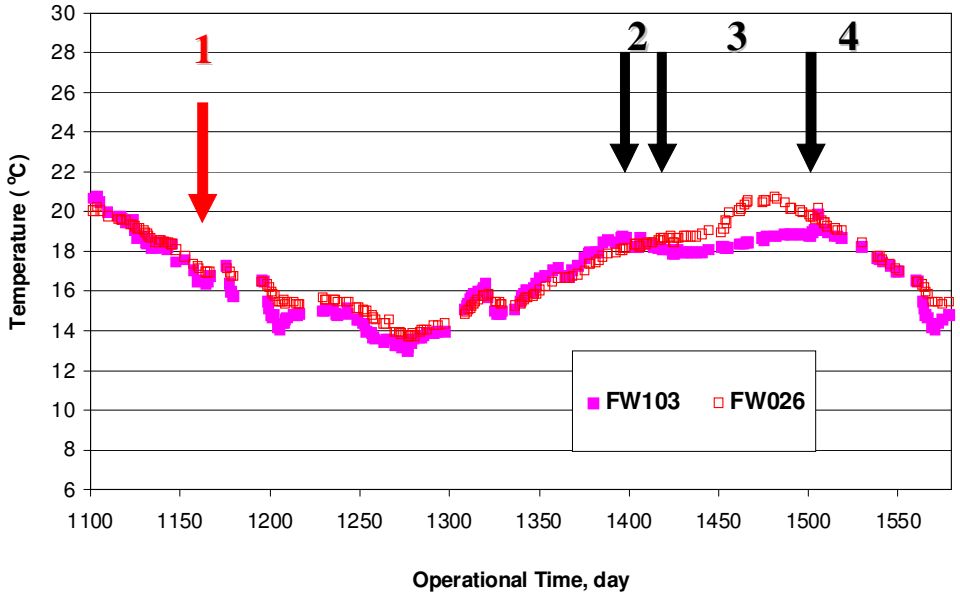

FIGURE S5. Changes in groundwater temperature during the study period. Numbered arrows indicate dates for (1) baseline measurements (Day 166); (2) controlled nitrate addition (Days 1398-1419); (3) Exposure of the reduced inner loop to source zone groundwater (Days 1420-1496); and (4) Re-reduction of the subsurface through weekly ethanol injections (Days 1497-1578).

11. Uranium distribution between aqueous and solid phase.

The uranium distribution between aqueous and solid phases was estimated based on the concentration and groundwater and uranium content in sediments. The subsurface porosity is assumed as 30% and the average specific gravity of sediments is 2.5 g cm^{-3}. Before remediation test, U concentrations in groundwater varied from 30-60 mg L^{-1} (126-252 µM) and sediment core samples had U content between 200-400 mg kg^{-1}. The estimated results indicated that approximately 2.5-5.0% was in aqueous phase. After biostimulation, 0.001% or less of U was in aqueous phase. After reoxidation, the distribution of U in aqueous phase was increased slightly but >99.99 of U was still in solid phase.

TABLE S4. Estimated uranium distribution

Monitoring Well	Day	Status	Groundwater		Sediments	
			U μM	%Total U	U mg/kg	% Total U
FW101-2	1202	R	0.14	0.001	555	99.999
	1490	O	0.82	0.048	691	99.952
	1578	R	0.1	0.0005	840	99.999
FW101-3	1202	R	0.052	0.0002	935	99.999
	1490	O	0.59	0.0025	956	99.998
	1578	O	0.4	0.0022	733	99.998
FW102-2	1202	R	0.097	0.0009	465	99.999
	1490	O	0.3	0.0043	284	99.996
	1578	R	0.13	0.002	264	99.998
FW102-3	1202	R	0.36	0.001	1404	99.999
	1490	O	0.86	0.0019	1814	99.998
	1578	R	0.11	0.0003	1793	99.999
Average	Before	O	252	2.51	400	97.49
	Before	O	252	4.89	200	95.11
	Before	O	126	1.27	400	98.73
	Before	O	126	2.51	200	97.49

Note: R=reduced; O=oxidized

Literature Cited

Cole, J.R.; Wang, Q.; Cardenas, E.; Fish, J.; Chai, B.; Farris, R.J.; Kulam-Syed-Mohideen, A.S.; McGarrell, D.M.; Marsh, T.; Garrity, G.M.; Tiedje, J.M. The Ribosomal Database Project: improved alignments and new tools for rRNA analysis. *Nucleic Acids Research*, **2009**, 37(Database issue):D141-D145.

DeSantis, T.Z.; Hugenholtz, P.; Keller, K.; Brodie, E.L.; Larsen, N.; Piceno, Y.M.; Phan, R.; Andersen, G.L. NAST: a multiple sequence alignment server for comparative analysis of 16S rRNA genes. *Nucleic Acids Research*, **2006**, 34(Web Server issue):W394-W399.

Kemner, K. M.; Kropf, A. J.; Bunker, B. A. A low-temperature total electron yield detector for X-ray absorption fine structure spectra. *Rev. Sci. Instrum.* **1994**, 65, 3667-3669.

Lane D. J. 16S/23S rRNA sequencing. In: *Nucleic Acid Techniques in Bacterial Systematics*; Stackebrandt, E.; Goodfellow, M.; Eds; John Wiley & Sons, Chichester, England, 1988, pp 115–147.

Lide, D.R. CRC Handbook of chemistry and physics, 71st Edition. 1991, pp5-16 to 5-59. CRC Press, Boca Raton, USA.

Luo, J; Wu, W.M.; Carley, J.; Ruan, C.; Gu, B.; Jardine, P.M.; Criddle, C.S; Kitanidis, P. K. Hydraulic performance analysis of a multiple injection-extraction well system. *J. Hydrol*. **2007**, 336, 294-302.

Muyzer, G.; Brinkhoff, T.; Nübel, U.; Santegoeds, C.; Schäfer, H.; Wawer, C. (1998) Denaturing gradient gel electrophoresis (DGGE) in microbial ecology. In: *Molecular microbial ecology manual*. Akkermans, A.D.L.; Elsas, J.D.V.; Bruijn, F.J.d.; Eds; Dordrecht; The Netherlands; Kluwer Academic Publishers;1998, pp1-27.

Newville, M. IFEFFIT: Interactive EXAFS analysis and FEFF fitting. *J. Synch. Rad*. **2001**, 8, 322-324.

O'Loughlin, E. J.; Kelly, S. D.; Cook, R. E.; Csencsits, R.; Kemner, K. M. Reduction of uranium(VI) by mixed iron(II)/iron(III) hydroxide (green rust): Formation of UO2 nanoparticles. *Environ. Sci. Technol*. **2003**, 37, 721-727.

Ravel, B.; Newville, M. ATHENA, ARTEMIS, HEPHAESTUS: Data analysis for X-ray absorption. *J. Synch. Rad*. **2005**, 12, 537-541.

Segre, C. U.; Leyarovska, N. E.; Chapman, L. D.; Lavender, W. M.; Plag, P. W.; King, A. S.; Kropf, A. J.; Bunker, B. A.; Kemner, K. M.; Dutta, P.; Druan, R. S.; Kaduk, The MRCAT insertion device beamline at the Advanced Photon Source. *J. Synchrotron Rad. Inst*. **2000**, CP521, 419-422.

Stern, E. A.; Heald, S. M. X-ray filter assembly for fluorescence measurements of x-ray absorption file structure .*Rev. Sci. Instrum.* **1979**, *50*, 1579-1583.

Thauer, R.K.; Jungermann, K.; Decker, K. Energy conservation in chemotrophic anaerobic bacteria. *Bacteriol. Rev.* **1977**, 41, 100-180.

Wang, Q.; Garrity, G.M.; Tiedje, J.M.; Cole, J.R. Naive Bayesian Classifier for Rapid Assignment of rRNA Sequences into the New Bacterial Taxonomy. *Appl. Environ. Microbiol*. **2007**, 73, 5261-5267.

Wu., W-M.; Carley, J.; Gentry, T.; Ginder-Vogel, M.A.; Fienen, M.; Mehlhorn, T.; Yan, H.; Carroll, S.; Nyman, J.; Luo, J.; Gentile, M.E.; Fields, M.W.; Hickey, R.F.; Watson, D.; Cirpka, O.A.; Fendorf, S.; Zhou, J.; Kitanidis, P.; Jardine, P.M.; Criddle, C.S. Pilot-scale in situ bioremediation of uranium in a highly contaminated aquifer. 2: U(VI) reduction and geochemical control of U(VI) bioavailability. *Environ. Sci. Technol*. **2006**, 40, 3986-3995.

Wu, W.-M., Carley,J.; Luo, J.; Ginder-Vogel, M.A.; Cardenas, E.; Leigh, M.B.; Hwang, C.; Kelly, S.D.; Ruan, C.; Wu, L.; Van Nostrand, J. ; Gentry, T. ; Lowe, K. ; Mehlhorn, T. ; Carroll, S. ; Luo, W.; Fields, M.W. ; Gu, B. ; Watson, D. ; Kemner, K.M. ; Marsh, T. ; Tiedje, J. ; Zhou, J. ; Fendorf, S. ; Kitanidis, P.K. ; Jardine, P.M. ; Criddle, C.S. *In situ* bioreduction of uranium (VI) to submicromolar levels and reoxidation by dissolved oxygen. *Environ. Sci. technol*. **2007**, 41, 5716-5723.